

AN EXPERIMENTAL COMPARISON OF REAL TIME PERFORMANCES OF NONLINEAR CONTROL SCHEMES ON A 2-DOF HELICOPTER

Yusuf Buğday¹
TOBB University
Ankara, Turkey

Mehmet Önder Efe²
Hacettepe University
Ankara, Turkey

ABSTRACT

Two-degrees-of-freedom (2-dof) helicopters are widely used test platforms in control laboratories due to their high non-linearity and the coupling between axial motions. The computer assisted structure provides a rapid prototyping environment for testing the designed approaches. This paper presents an experimental comparison of fuzzy control, sliding mode control, backstepping control and passivity-based sliding mode control on a 2-dof helicopter. The design steps are given and the comparison is done under few metrics quantifying the steady state and transient qualities for each embedded software approach. The contribution of the paper is to unfold the application specific issues of frequently experimented control schemes as well as to demonstrate the prominent results of passivity based design oriented control software comparatively to control platform developers and practitioners.

INTRODUCTION

The notion of nonlinear control system design has been an interesting topic for years and the main reason for that has been the diversity of dynamical forms and associated solution methods. Despite the linear control courses convey a comprehensive curriculum to the practicing engineers; it is not at that maturity for the nonlinear control applications. Experimental comparison works, in this sense, fills an important gap as there are issues of nonlinear and coupled dynamics, actuation impreciseness, and high performance expectations and so on. This paper aims to address this goal to the extent covering several popular nonlinear control laws implemented on a 2-dof helicopter system, also called twin-rotor system. The paper treats these schemes as software components as the methods are all implemented on computer platforms having the capability of handling different levels of computational intensity that change from one approach to another.

In a study done in past, a comparison has been made between intelligent and conventional control methods through simulations and the accuracy of intelligent systems is emphasized by [Juang et al., 2008]. In the study of [Ahmad et al., 2003], a linear quadratic Gaussian control is realized for a real time tracking application on a twin-rotor system, and as the result, high-amplitude oscillations are observed in the steady state. Two works focusing on a laboratory type helicopter consider nonlinear L_2 and H_∞ approaches and present successful results in a real time tracking, [Lopez-Martinez et al., 2007; Lopez-Martinez et al., 2005]. [Shaik

¹ Researcher, Email: josephwheat@gmail.com

² Professor, Email: onderefe@gmail.com

and Purwar, 2009] realized a nonlinear state observer design for twin rotor system, and the study of [Juang et al., 2008] utilizes a PID reinforced with genetic algorithm for the control of 2-DOF helicopter.

The first approach considered in this paper is fuzzy control which is a control scheme based on the fuzzy logic, which is a method exploiting the verbal and local descriptions of maps through fuzzy sets, [Mendel, 2001]. A real time implementation study on a 2-dof helicopter proposes a hybrid control scheme consisting of both fuzzy and PID techniques, and the performance improvement is demonstrated when the fuzzy approach is incorporated into the control system [Rahideh and Shaheed, 2009]. Two studies utilize fuzzy approach to model the system by Takagi-Sugeno fuzzy modeling method with parallel distributed compensation and design the controllers through this fuzzy model of 2-dof helicopter [Yu, 2007; Agudelo et al., 2007]. The study of [Tao et al., 2010], presents a sliding mode controller benefiting from fuzzy logic for a twin rotor system.

Second method considered for comparison in this paper is sliding mode control (SMC) postulated by Emelyanov in early 1950s. SMC is an elegant control scheme that is known for its insensitivity against disturbances and uncertainties. A comprehensive survey providing the state of the art of recent developments in SMC have been presented by [Yu and Kaynak, 2009]. A thorough treatment of the approach for electromechanical systems is described in [Utkin et al., 2009]; and many studies highlighting the new directions and improvements in SMC are reported, such as fractional fuzzy adaptive SMC in [Efe, 2008], or the adaptive fuzzy SMC used for synchronization of two different chaotic systems by [Roopaei and Jahromi, 2008]. Su et al. realized the control twin rotor system by utilising inverse complementary and terminal SMCs, [Su et al., 2002].

The third control approach utilized in this work is backstepping which has been proposed by Kokotovic and employed by numerous researchers during the last few decades, The references [Bridges et al., 1995; Krstic et al., 1995; Freeman, 2008] are the key contributions to the backstepping method. In [Frazzoli et al., 2000] designs a tracking controller for a small scale helicopter using backstepping technique and provides simulation results. Another work establishes a backstepping controller for a quadrotor type helicopter through the dynamics described in Lagrangian form [Das et al., 2009]. An adaptive backstepping controller is used in [Yang and Hsu, 2009] considering unknown system parameters, and the designed controller is tested experimentally on the twin-rotor system considered here.

The last scheme is designed using the passivity formalism. The extension of passivity approach in control theory, called passivity-based control (PBC), benefits from the results of Lyapunov stability theory. A remarkable work discussing the issues in passivity, backstepping and SMC approaches is by Khalil, [23]. A reference book by Ortega considers the control of Euler-Lagrange based models including electromechanical systems, such as manipulators, electric machines, and power converters, by using PBC, [Ortega, 1998]. In [Koshkouei, 2008], Koshkouei proposes a passivity-based sliding mode control (PB-SMC) scheme including linear and adaptive nonlinear variants. Ma et al. presents a PB-SMC strategy that is applied to control a current-source inverter, [Ma et al., 2009]. A recent trend in the applications of passivity based design is the blending of the approach with other techniques. Wang and Chen provide a PB-SMC designed to control the position of an induction motor and demonstrates experimental results, [Wang and Chen, 2005].

This paper is organized as follows. The second section gives the derivation of the dynamic model of the helicopter, the third section presents the fuzzy control of the system, the sliding mode control of the helicopter is focused on in the fourth section, backstepping control technique is elaborated in the fifth section, passivity based sliding mode control scheme is studied as the last scheme in section six. The concluding remarks are given at the end of the paper.

DYNAMIC MODEL OF 2-DOF HELICOPTER SYSTEM

2-DOF helicopter utilized in this work consists of a fuselage that is equipped with two different types of DC motors with propellers and mounted on a fixed base as shown in Figure 1. The main propeller of helicopter controls the pitch angle (θ) defined as the angle between helicopter nose and horizontal. The rotational position of helicopter around the fixed base is defined as yaw angle (ψ) and controlled by the tail propeller. Numerical data are associated to these angles are measured by two encoders mounted on the fixed base and transmitted to Matlab/Simulink[®] environment on a desktop PC via a data acquisition board and a PCI card in real time. The software development platform is based on Matlab[®] and the approaches yet to be discussed are all prototyped in this environment.

In all experiments presented, the initial and minimum value of pitch angle is -40.5 degrees and the maximum is restricted to 35 degrees ($\theta_0 = -40.5^\circ$, $-40.5^\circ \leq \theta \leq 35^\circ$). Initial position of yaw angle is always accepted as the zero degree position and the slip ring mechanism of fixed base allows the helicopter to rotate freely over 360 degrees ($\psi_0 = 0^\circ$, $|\psi| \leq 360^\circ$). Positive directions of motion are defined as clockwise rotation for yaw angle and upwards movement of the helicopter nose for pitch angle as shown in Figure 2. The pitch motor is called the main motor and the yaw motor is called the tail motor also.

In the literature, there are several researches that propose models for 2-DOF helicopter system through analytical and soft computing methods such as [Toha and Tokhi, 2010; Subudhi and Jena, 2009]. The mathematical models of systems play a leading role in the success of model based controllers. Correspondingly the way chosen to obtain the mathematical model has considerable effects on the performance of a closed loop controller based on the available model. In this study, the equations of motion of the system are derived by using the Lagrangian method. A comparison of the Newtonian and Lagrangian models of a 2-DOF helicopter, which includes all steps of modelling, is presented by [Rahideh and Shaheed, 2006] and it is claimed that the Lagrangian method contains the representational details better.

The Euler-Lagrange equations of the system are

$$\frac{d}{dt} \frac{\partial L}{\partial \dot{\theta}} - \frac{\partial L}{\partial \theta} = Q_1 \quad (1)$$

$$\frac{d}{dt} \frac{\partial L}{\partial \dot{\psi}} - \frac{\partial L}{\partial \psi} = Q_2 \quad (2)$$

where L , called Lagrangian variable, is the difference between potential and kinetic energy of the system. Generalized coordinates are given by $q = [\theta \ \psi \ \dot{\theta} \ \dot{\psi}]^T$ and generalized forces are given by (3)-(4), respectively

$$Q_1 = \tau_p(V_{m,p}, V_{m,y}) - B_p \dot{\theta} \quad (3)$$

$$Q_2 = \tau_y(V_{m,p}, V_{m,y}) - B_y \dot{\psi} \quad (4)$$

where B_p and B_y are viscous rotary frictions acting on pitch and yaw movements. The torques, τ_p and τ_y , are functions of both voltages applied to pitch and yaw motors. Due to the coupling between the axial motions, the voltage applied to one axis is seen also in the torque expression of the other axis, which is clear in the below equations.

$$\tau_p(V_{m,p}, V_{m,y}) = K_{pp}(\theta)V_{m,p} + K_{py}V_{m,y} \quad (5)$$

$$\tau_y(V_{m,p}, V_{m,y}) = K_{yp}V_{m,p} + K_{yy}V_{m,y} \quad (6)$$

In above, the subscripts p and y denote the pitch and yaw axes respectively and other than K_{pp} , the coefficients are constant. Due to high nonlinearity, we develop a model for K_{pp} experimentally which is a second order polynomial of θ given in (7). Other plant parameters are listed in Table 1 as provided by the manufacturer of the system.

$$K_{pp}(\theta) = -9.535 \cdot 10^{-6} \theta^2 - 7.281 \cdot 10^{-4} \theta + 0.1624 \quad (7)$$

After straightforward mathematical manipulations detailed in [Quanser Inc., 2006], nonlinear ordinary differential equations of the motion are obtained as below.

$$(J_p + m_h l_{cm}^2) \ddot{\theta} = K_{pp}(\theta) V_{m,p} + K_{py} V_{m,y} - B_p \dot{\theta} - m_h l_{cm}^2 \sin(\theta) \cos(\theta) \dot{\psi}^2 - m_h g l_{cm} \cos(\theta) \quad (8)$$

$$(J_y + m_h l_{cm}^2 \cos(\theta)^2) \ddot{\psi} = K_{yp} V_{m,p} + K_{yy} V_{m,y} - B_y \dot{\psi} - 2m_h l_{cm}^2 \sin(\theta) \cos(\theta) \dot{\theta} \dot{\psi} \quad (9)$$

State space model of the system, used frequently in model based controller design, is defined as (10) through (13) by defining the positions and velocities as the state variables.

$$\begin{aligned} \dot{x}_1 &= x_2 \\ \dot{x}_2 &= f(\theta, \psi) + g(\theta)u \\ y &= x_1 \end{aligned} \quad (10)$$

where

$$x_1 = \begin{bmatrix} \theta \\ \psi \end{bmatrix} \quad x_2 = \begin{bmatrix} \dot{\theta} \\ \dot{\psi} \end{bmatrix} \quad u = \begin{bmatrix} V_{m,p} \\ V_{m,y} \end{bmatrix} \quad (11)$$

$$g(\theta) = \begin{bmatrix} \frac{K_{pp}}{J_p + m_h l_{cm}^2} & \frac{K_{py}}{J_p + m_h l_{cm}^2} \\ \frac{K_{yp}}{J_y + m_h l_{cm}^2 \cos(\theta)^2} & \frac{K_{yy}}{J_y + m_h l_{cm}^2 \cos(\theta)^2} \end{bmatrix} \quad (12)$$

$$f(\theta, \psi) = \begin{bmatrix} \frac{-B_p \dot{\theta} - m_h l_{cm}^2 \sin(\theta) \cos(\theta) \dot{\psi}^2 - m_h g l_{cm} \cos(\theta)}{J_p + m_h l_{cm}^2} \\ \frac{-B_y \dot{\psi} - 2m_h l_{cm}^2 \sin(\theta) \cos(\theta) \dot{\theta} \dot{\psi}}{J_y + m_h l_{cm}^2 \cos(\theta)^2} \end{bmatrix} \quad (13)$$

Table 1: Parameters describing the 2-DOF Helicopter

Symbol	Explanation	Value
B_p	Viscous friction on pitch motion	0.8000 <i>N/V</i>
B_y	Viscous friction on yaw motion	0.3180 <i>N/V</i>
g	Acceleration due to gravity	9.8100 <i>m/s²</i>
J_p	Moment of inertia about pitch axis	0.0384 <i>kg · m²</i>
J_y	Moment of inertia about yaw axis	0.0432 <i>kg · m²</i>
m_h	Mass of helicopter	1.3872 <i>kg</i>
r_p	Distance from pivot to pitch motor	0.1969 <i>m</i>
r_y	Distance from pivot to yaw motor	0.1683 <i>m</i>
l_{cm}	Distance from pivot to center of mass	0.1857 <i>m</i>
K_{pp}	Relation between pitch motor voltage and the torque acting on pitch axis	See text <i>N · m/V</i>
K_{py}	Ratio between pitch motor voltage and the torque acting on yaw axis	0.0068 <i>N · m/V</i>
K_{yp}	Ratio between yaw motor voltage and the torque acting on pitch axis	0.0219 <i>N · m/V</i>
K_{yy}	Ratio between yaw motor voltage and the torque acting on yaw axis	0.0720 <i>N · m/V</i>

The control problem is to maintain the necessary angles by appropriately scheduling the motor voltages denoted by $V_{m,p}$ and $V_{m,y}$. In the sequel, we describe three schemes with a comparison of the approaches experimented in real time.

FUZZY CONTROL

Fuzzy control is a rule based control technique that allows controlling processes through the descriptions of system behavior in terms of linguistic variables constituting a rule structure. Crisp inputs are mapped to crisp outputs by an appropriately designed inference system as prescribed by the rule base. The flow of information through the fuzzy controller undergoes fuzzification and defuzzification stages enabling the designer to make choices from a diverse set of possibilities. Designing the resolution of the rule base and the type of inference are other flexibilities provided to the design engineer. The underlying philosophy is to incorporate the experiences of an expert into the design or to come up with a design that is mostly based on the physics of the process, utilizing the possibilities available in the domain of linguistic labels. The reason motivating us to experiment fuzzy control technique is mainly because of the appropriateness of the behavior of the helicopter system. This paper aims to accomplish a tracking task by two individual controllers for pitch and yaw angles. In this case, robustness of controllers is a vital necessity because a movement in an axis reverberates as a disturbance on the other axis, which emphasized the coupling effect in between the axes. Input output relations of the designed Sugeno type fuzzy controllers can be given in the form of fuzzy basis functions as in (14).

$$u_{(p,y)} = \frac{\sum_{i=1}^R y_{i;(p,y)} \prod_{j=1}^m \mu_{ij;(p,y)}(e_{j;(p,y)})}{\sum_{i=1}^R \prod_{j=1}^m \mu_{ij;(p,y)}(e_{j;(p,y)})} \quad (14)$$

where $m = 2$ in our case and the subscript (p,y) denotes that the controller belongs to either pitch angle or yaw angle. The parameters $e_{1,p}$ and $e_{1,y}$ are angular position errors, $e_{2,p}$ and $e_{2,y}$ are angular velocity errors. $\mu_{ij,p}$ and $\mu_{ij,y}$ are membership functions of pitch and yaw angles, respectively. Both controllers are established with $R = 25$ rules described via triangular membership functions. The inputs to the pitch angle controller are $(e_{1,p}, e_{2,p})$ and that for the yaw angle controller are $(e_{1,y}, e_{2,y})$. The control signals (u_p, u_y) , driving the motors, are obtained in Volts as crisp output from (14). Rule bases of pitch and yaw angles have the structure given as below.

IF $e_{1,p} \in P_p$ and $e_{2,p} \in Q_p$ **THEN** $u_p = y_{i,p}$ $i = 1, 2, \dots, R$

IF $e_{1,y} \in P_y$ and $e_{2,y} \in Q_y$ **THEN** $u_y = y_{i,y}$ $i = 1, 2, \dots, R$

For producing necessary control signals driving the main motor, both pitch error and pitch position are essential. More explicitly, main motor needs a higher voltage level to settle the helicopter nose at a higher position than lower positions in steady state. This shows that the needed control surface is not symmetric. Consequently, defuzzifier parameters of pitch controller ($y_{i,p}$) are produced through an angle-voltage characteristic shown in Figure 3 determined experimentally. This characteristic is obtained as a result of a set of open loop tests and it shows the steady state pitch angle value for an applied input voltage to the main motor of the helicopter. An approximation is performed with a sixth order polynomial given in (15) and defuzzifier parameters are chosen after numerous experiments carried out on the system and the content is given in (16). In (16), different from the standard practice of fuzzy logic control, a nonlinear bias, $p(x)$, is utilized to provide the necessary asymmetry mentioned above.

$$p(x) = 1.153 \cdot 10^{-9} \theta^6 + 6.621 \cdot 10^{-8} \theta^5 - 5.047 \cdot 10^{-7} \theta^4 - 6.48 \cdot 10^{-5} \theta^3 - 0.00144 \theta^2 + 0.08096 \theta + 15.79 \quad (15)$$

$$y_p = p(x) + [10 \ 9 \ 8 \ 6 \ -1.5 \ 4.5 \ 3 \ 2 \ 0 \ -2.5 \ 2 \ 0.5 \ 0 \ -0.4 \ -1.5 \ +1.5 \ -0.3 \ -1.5 \ -2.5 \ -4 \ 1 \ -5 \ -8 \ -9 \ -10]^T \quad (16)$$

Contrariwise, defuzzifier parameters of the yaw controller ($y_{i,y}$) are selected directly as constant values based on the gained experimental insight and the chosen values are given in (17), where the induced control surface is symmetric as the parameters and the membership functions are symmetric.

$$y_y = [-15 \quad -14 \quad -13 \quad -12 \quad -11 \quad -13 \quad -11 \quad -9 \quad -8 \quad -7 \quad -9 \quad -6.5 \quad -6 \quad -5.5 \quad -3 \quad -5 \quad -4 \quad -3 \quad -1.2 \quad -0.6 \quad -3.5 \quad -1.5 \quad -1 \quad -0.8 \quad -0.5]^T \quad (17)$$

The selections are done in the range of input voltage limits of the motors, i.e. ± 24 Volts for the main motor and ± 15 Volts for the tail motor. Since the gravitational force (F_g) is sufficient to reduce the pitch angle, there is no need to quantify the main motor input with negative values. Accordingly, (16) is adjusted so as to produce always positive valued outputs. Likewise, positive voltage values are not used for the tail motor due to the force stemming from the coupling between the axes.

Membership functions ($\mu_{ij,p}$, $\mu_{ij,y}$), seen in (14) are depicted in Figure 4. The mathematical descriptions of the membership functions are given in (18) through (22) corresponding to the linguistic variables labeled as Big Negative (BN), Negative (N), Zero (Z), Positive (P) and Big Positive (BP).

$$\mu_{BN}(x) = \max\left(\min\left(-\frac{x+L}{L_B-L}, 1\right), 0\right) \quad (18)$$

$$\mu_N(x) = \max\left(\min\left(-\frac{x}{L}, \frac{x+L_B}{L_B-L}\right), 0\right) \quad (19)$$

$$\mu_Z(x) = \max\left(\min\left(1+\frac{x}{L}, 1-\frac{x}{L}\right), 0\right) \quad (20)$$

$$\mu_P(x) = \max\left(\min\left(\frac{x}{L}, -\frac{x-L_B}{L_B-L}\right), 0\right) \quad (21)$$

$$\mu_{BP}(x) = \max\left(\min\left(\frac{x-L}{L_B-L}, 1\right), 0\right) \quad (22)$$

The definitions of the parameters L and L_B can be seen in Figure 4, the chosen values of these parameters are listed in Table 2. The membership functions are then implemented in Matlab/Simulink[®] environment with these settings. Thus, the design of the fuzzy control system is completed and the control surfaces obtained from the fuzzy controller dedicated to pitch and yaw angles are constructed as illustrated in Figure 5 and Figure 6.

Table 2: L and L_B selections

Parameter	Explanation	Value
L for;	Position error of pitch angle	0.5 degree
	Velocity error of pitch angle	1.5 degree/sec
	Position error of yaw angle	0.5 degree
	Velocity error of yaw angle	3 degree/sec
L_B for;	Position error of pitch angle	10 degree
	Velocity error of pitch angle	25 degree/sec
	Position error of yaw angle	5 degree
	Velocity error of yaw angle	20 degree/sec

For real time tracking applications, reference path is chosen as a mixture of a sine wave trajectory followed by a square wave one. This choice is deliberate as we would like to see the performance of the system when the reference signals are differentiable and when they contain sharp changes. As seen in Figure 3, the problematic region of pitch axis is between 15 and 25 degrees. To make the tracking more challenging, the amplitude of reference path is chosen as 20 degrees and tracking of both pitch and yaw angles are performed simultaneously. Real time implementation results are given in Figures 7-8 for pitch and yaw angles, respectively. According to the results, the states follow their desired values accurately, the response during the transient regime and the steady state regimes are seen acceptable. The fuzzy logic controller is able to synthesize the control signals having some degrees of complexity seen from the time evolution of the applied motor voltages. Expectedly, the conclusion drawn from this section is the necessity to some degree of expert knowledge to refine the controller for a better closed loop performance.

SLIDING MODE CONTROL

Sliding mode control is a widely known nonlinear control scheme that is preferred because of its robustness against unmodeled dynamics and disturbances caused by different kinds of internal and external factors. The methodology of SMC guides the vector of chosen states from any initial point of the phase space to a prespecified and particularly designed subspace, which is a global attractor due to the design and once the trajectories get trapped to it, the motion afterwards takes place in the vicinity of it. The errors gradually converge to the origin and the control scheme borrows its name from the sliding behavior arising along the designed subspace. For a tracking implementation, it is common to choose the states as the tracking error and its derivatives of order up to a specific value. Having this in mind, referring to the state space model described in (10) through (13), error components are defined as below.

$$e_0(t) = \int (x_1 - r_1) dt \quad (23)$$

$$e_1(t) = x_1 - r_1 \quad (24)$$

$$e_2(t) = x_2 - r_2 \quad (25)$$

where all variables on the left hand side are 2×1 matrices and, r_1 and r_2 , respectively, denote the reference paths for pitch and yaw angles and their derivatives are defined as

$$r_1 = [\theta_d \quad \psi_d]^T, \quad \dot{r}_1 = r_2 \quad (26)$$

Furthermore, r_2 is assumed to be differentiable for the design phase. Resetting of the integration is utilized in real time applications. The integrator is reset when the desired value is reached, i.e. $e_1=0$. Such a resetting scheme prevents the potential oscillations and overshoots during the implementations. Switching function to derive the control laws is defined as

$$\sigma = e_2 + \lambda_1 e_1 + \lambda_0 e_0 \quad (27)$$

$$\lambda_0 = \begin{bmatrix} \lambda_{0,\theta} & 0 \\ 0 & \lambda_{0,\psi} \end{bmatrix}, \quad \lambda_1 = \begin{bmatrix} \lambda_{1,\theta} & 0 \\ 0 & \lambda_{1,\psi} \end{bmatrix} \quad (28)$$

Since we need a stable locus described by $\sigma = 0$, the values seen above are chosen such that $s^2 + \lambda_1 s + \lambda_0 = 0$ is Hurwitz, where s is the Laplace variable. Calculating the time derivative of the switching function lets us have the following:

$$\begin{aligned} \dot{\sigma} &= \dot{e}_2 + \lambda_1 \dot{e}_1 + \lambda_0 \dot{e}_0 \\ &= \dot{x}_2 - \dot{r}_2 + \lambda_1 e_2 + \lambda_0 e_1 \\ &= f(\theta, \psi) + g(\theta)u - \dot{r}_2 + \lambda_1 e_2 + \lambda_0 e_1 \end{aligned} \quad (29)$$

In order to establish the reaching regime in the phase space, we choose the control signal such that the reaching law in (30) is satisfied.

$$\dot{\sigma} := -\Phi \operatorname{sgn}(\sigma) \quad (30)$$

where

$$\Phi = \begin{bmatrix} \Phi_\theta & 0 \\ 0 & \Phi_\psi \end{bmatrix}, \quad \Phi_\theta > 0, \quad \Phi_\psi > 0 \quad (31)$$

This particular selection implies that the closed loop system is Lyapunov stable. The proof is straightforward. For such a Φ , reaching law guarantees the convergence of any initial value of the error vector to the switching subspace characterized by $s = 0$, which is stable by the design, [Ertuğrul et al., 1996; Tokat et al., 2009]. The response after hitting the switching surface exhibits a certain degree of robustness and invariance properties as it is confined to the switching subspace. Solving (29) and (30) for u gives the control law

$$u(t) = g(\theta)^{-1} (-f(\theta, \psi) + \dot{r}_2 - \lambda_1 e_2 - \lambda_0 e_1 - \Phi \operatorname{sgn}(\sigma)) \quad (32)$$

where the nonsingularity of $g(\theta)$ is a necessity. The critical value of K_{pp} making $g(\theta)$ singular is 0.00207, yet this variable is always greater than the critical value.

Once the sliding regime starts, the control law above becomes quite sensitive to the value of σ , which is small in magnitude and naturally noisy. In this regime, if no precautions are taken, the sign of the switching variable is determined mainly by the noise and this causes severely corrupted control signals, called chattering in the literature. In order to avoid this, the sign function is approximated by a continuous function providing a smooth transition around origin yet introducing a tiny boundary layer around the sliding subspace.

$$\text{sgn}(\sigma) \cong \frac{\begin{bmatrix} \sigma_\theta \\ |\sigma_\theta| + \delta_\theta \\ \sigma_\psi \\ |\sigma_\psi| + \delta_\psi \end{bmatrix}}{\begin{bmatrix} \sigma_\theta \\ |\sigma_\theta| + \delta_\theta \\ \sigma_\psi \\ |\sigma_\psi| + \delta_\psi \end{bmatrix}}, \quad \delta_{\theta,\psi} > 0 \quad (33)$$

During the real time implementation, the term in (33) is saturated as given by $\min\left(\max\left(-0.1, \frac{\sigma_\psi}{|\sigma_\psi| + \delta_\psi}\right), 0.5\right)$. This prevents the overshoots arising right after the falling and rising

edges of square reference without affecting the stability conclusion of the closed loop system. As mentioned previously, the produced control signals are saturated to their physical limits, which is hard constraint. The controller in (32) is implemented in Matlab/Simulink[®] platform and the reference signal is chosen the same as in the previous section. After a number of experiments, the parameters to be selected by the designer are fixed as listed in Table 3. Real time implementation results are depicted in Figures 9-10 for pitch and yaw angles, respectively. It is seen that the helicopter followed the desired trajectories with an acceptable error margin, however there are high frequency fluctuations in the control signals indicating some amount of chattering available in the phase space behavior shown in Figures 11-12. According to the results obtained in the phase space, it is seen that the errors hit the sliding surface and remains on it. The errors finally converge to the origin. The results in Figures 11-12 illustrate different temporal intervals so as to make it visible what happens initially, and what happens for continuous and discontinuous reference profiles.

Table 3: Parameter Settings of SMC Scheme

Paramete	Explanation	Value
r		
Φ_θ	Reaching law parameter of pitch angle	20
Φ_ψ	Reaching law parameter of yaw angle	10.5
$\lambda_{0,\theta}$	The slope parameter of error integration of pitch angle	0.15
$\lambda_{0,\psi}$	The slope parameter of error integration of yaw angle	1
$\lambda_{1,\theta}$	The slope parameter of error of pitch angle	0.8
$\lambda_{1,\psi}$	The slope parameter of error of yaw angle	5
δ_θ	Signum smoothing parameter of pitch angle	0.25
δ_ψ	Signum smoothing parameter of yaw angle	0.2

The conclusions drawn in this scheme are the presence of high frequency components in the control signal as a price paid for the robustness against disturbances and parameter uncertainties. Switching nature of the control law makes is vulnerable to noise yet it makes the overall control system robust.

BACKSTEPPING CONTROL

Backstepping is one of the frequently experimented nonlinear control strategies in the literature. The design philosophy is based on the use of each state variable to stabilise another, organized in a chain structure from the input to output, thus, the stabilization of every state variable is ensured individually. The controller design procedure of backstepping method aims to construct a recursive algorithm defining virtual states to make the control law obtainable.

As in the previous sections, we have designed two individual controllers for pitch and yaw motions by referring to the state space model defined in (10) through (13). The reference signal (r) definitions are the same as in the previous section. The tracking problem can be transformed to a stabilization problem by choosing the following intermediate variables.

$$z_1 := x_1 - r_1 \quad (34)$$

$$z_2 := x_2 - r_2 - \Lambda \quad (35)$$

where Λ is a variable yet to be selected to meet the stability criterion. Choosing

$$V_1 = \frac{1}{2} z_1^T z_1 \quad (36)$$

as the Lyapunov function candidate and taking its time derivative can be manipulated as given in (37).

$$\begin{aligned} \dot{V}_1 &= z_1^T \dot{z}_1 \\ &= z_1^T (\dot{x}_1 - \dot{r}_1) \\ &= z_1^T (x_2 - r_2) \\ &= z_1^T (z_2 + \Lambda) \end{aligned} \quad (37)$$

where Λ is chosen as described by (38).

$$\Lambda := -k_1 \text{sat}(z_1), \quad k_1 = \text{diag}(k_{1,\theta} \quad k_{1,\psi}), \quad k_{1,\theta} > 0, k_{1,\psi} > 0 \quad (38)$$

The term $\text{sat}(z_1)$ used above corresponds to the saturation function described as given below.

$$\text{sat}(z_1) = \begin{cases} \varphi_h & \text{if } z_1 > \varphi_h \\ z_1 & \text{if } \varphi_l \leq z_1 \leq \varphi_h, \\ \varphi_l & \text{if } z_1 < \varphi_l \end{cases}, \quad \varphi_l = \begin{bmatrix} \varphi_{l,\theta} \\ \varphi_{l,\psi} \end{bmatrix}, \quad \varphi_h = \begin{bmatrix} \varphi_{h,\theta} \\ \varphi_{h,\psi} \end{bmatrix}, \quad \varphi_{l,\theta} < 0, \varphi_{l,\psi} < 0, \varphi_{h,\theta} > 0, \varphi_{h,\psi} > 0 \quad (39)$$

This Λ selection lets us have $\dot{V}_1 = -z_1^T k_1 \text{sat}(z_1) + z_1^T z_2$, the second term of which will be handled appropriately in the second step of the design. Now choose the following Lyapunov function;

$$V_2 = V_1 + \frac{1}{2} z_2^T z_2 \quad (40)$$

Ensuring the negativity of the expression in (40) guarantees the global stability in the coordinates described by the intermediate variables. Taking the time derivative of (40) yields the expressions in (41), where we see the external control variables explicitly.

$$\begin{aligned} \dot{V}_2 &= \dot{V}_1 + z_2^T \dot{z}_2 \\ &= -z_1^T k_1 \text{sat}(z_1) + z_1^T z_2 + z_2^T \dot{z}_2 \\ &= -z_1^T k_1 \text{sat}(z_1) + z_2^T z_1 + z_2^T \dot{z}_2 \\ &= -z_1^T k_1 \text{sat}(z_1) + z_2^T (z_1 + \dot{z}_2) \\ &= -z_1^T k_1 \text{sat}(z_1) + z_2^T (z_1 + \dot{x}_2 - \dot{r}_2 - \dot{\Lambda}) \\ &= -z_1^T k_1 \text{sat}(z_1) + z_2^T (z_1 + f(\theta, \psi) + g(\theta)u - \dot{r}_2 - \dot{\Lambda}) \end{aligned} \quad (41)$$

Equating the sum in the parentheses to $-k_2 z_2$ as given below leads to the control law in (43).

$$z_1 + f(\theta, \psi) + g(\theta)u - \dot{r}_2 - \dot{\Lambda} := -k_2 z_2, \quad k_2 = \text{diag}(k_{2,\theta} \quad k_{2,\psi}), \quad k_{2,\theta} > 0, k_{2,\psi} > 0 \quad (42)$$

$$u = g(\theta)^{-1} (-f(\theta, \psi) + \dot{r}_2 - k_2 z_2 - z_1 - \dot{\Lambda}) \quad (43)$$

According to the definition in (39), we have $\dot{\Lambda} = \dot{z}_1$ when z_1 is in between or equal to the defined upper and lower bounds, otherwise $\dot{\Lambda} = 0$. The voltages applied to the motors are further saturated to their physical limits. The controller is realized in Matlab/Simulink[®] environment with the settings listed in Table 4. Trajectory tracking results are shown in Figures 13-14 for pitch and yaw angles respectively. As seen in the illustrations, the desired trajectories are followed in both directions accurately. The control signals are distinguishably clearer than those produced by the controllers considered so far and the tracking precision is satisfactorily good.

Table 4: Parameter settings of backstepping scheme

Paramete	Explanation	Value
r		
$k_{1,\theta}$	Coefficient of z_1 for pitch angle	3
$k_{1,\psi}$	Coefficient of z_1 for yaw angle	13
$k_{2,\theta}$	Coefficient of z_2 for pitch angle	40
$k_{2,\psi}$	Coefficient of z_2 for yaw angle	15.4
$\varphi_{l,\theta}$	Lower limit of $\text{sat}(z_1)$ for pitch angle	-0.1
$\varphi_{l,\psi}$	Lower limit of $\text{sat}(z_1)$ for yaw angle	-0.0175
$\varphi_{h,\theta}$	Upper limit of $\text{sat}(z_1)$ for pitch angle	0.116
$\varphi_{h,\psi}$	Upper limit of $\text{sat}(z_1)$ for yaw angle	0.035

PASSIVITY-BASED SLIDING MODE CONTROL

Passivity formalism has a wide range of applications in feedback control theory. Its connection with Lyapunov stability theory makes it an approach standing on a strong basis. The philosophy of passivity based control rests on the notions of passivity, zero state observability and Lyapunov stability. By using the storage function of passivity as a candidate Lyapunov function, a stability rule is obtained, additionally, if the zero state observability is fulfilled, the stability of the origin is ensured. Various methods, like SMC or backstepping design can be embedded into the passivity formalism to meet the prespecified performance criteria. In this section, a passivity-based controller is designed by utilizing the sliding mode approach.

Consider the system,

$$\begin{aligned}\dot{x} &= f(x) + g(x)u \\ y &= h(x)\end{aligned}\quad (44)$$

where f , g and h are smooth functions of the state, and suppose this system is

- i. passive with a positive definite storage function (V) and
- ii. zero-state observable.

The control law given as $u = -\Gamma(y)$, where Γ is any smooth function such that $\Gamma(0) = 0$ and $y^T \Gamma(y) > 0$ for all y other than zero, can stabilize the origin ($x = 0$) of system in (44). Furthermore, if the storage function (V) is radially unbounded, the system (44) can be globally stabilized by u . This well known passivity based control theorem is explained in detail by [Khalil, 2002].

In order to provide the simplicity of controller design process, in this section the helicopter system is considered as in (45) instead of the state space representation used before.

$$D(q)\ddot{q} + C(q, \dot{q})\dot{q} + B\dot{q} + G(q) = \tau \quad (45)$$

where the matrices of inertia (D), damping (C), viscous friction (B), gravity (G), applied torque (τ), state vector (q), voltage-torque ratio ($g(\theta)$) and the control input of motor voltages (u) are as given below.

$$q = \begin{bmatrix} \theta \\ \psi \end{bmatrix}, \quad g(\theta) = \begin{bmatrix} K_{pp}(\theta) & K_{py} \\ K_{yp} & K_{yy} \end{bmatrix}, \quad u = \begin{bmatrix} V_p \\ V_y \end{bmatrix} \quad (46)$$

$$D(q) = \begin{bmatrix} J_p + m_h l_{cm}^2 & 0 \\ 0 & J_h + m_h l_{cm}^2 \cos^2 \theta \end{bmatrix} \quad (47)$$

$$C(q, \dot{q}) = \begin{bmatrix} 0 & m_h l_{cm}^2 \sin \theta \cos \theta \dot{\psi} \\ -2m_h l_{cm}^2 \sin \theta \cos \theta \dot{\psi} & 0 \end{bmatrix} \quad (48)$$

$$B = \begin{bmatrix} B_p & 0 \\ 0 & B_y \end{bmatrix} \quad (49)$$

$$G(q) = \begin{bmatrix} m_h g l_{cm} \cos \theta \\ 0 \end{bmatrix} \quad (50)$$

$$\tau = g(\theta)u \quad (51)$$

The vector of tracking error is defined as $q_e = q - q_d$ where the desired position is designated with $q_d = [q_{d,\theta}, q_{d,\psi}]^T$. The dynamic equation of system (45) is written in the form below by using the q_e definition.

$$D(q)(\ddot{q}_e + \ddot{q}_d) + C(q, \dot{q})(\dot{q}_e + \dot{q}_d) + B(\dot{q}_e + \dot{q}_d) + G(q) = \tau \quad (52)$$

The terms which include the vector of error q_e are left alone in the left hand side of equation and consequently an error system is obtained.

$$D(q)\ddot{q}_e + C(q, \dot{q})\dot{q}_e + B\dot{q}_e = \tau - G(q) - D(q)\ddot{q}_d - C(q, \dot{q})\dot{q}_d - B\dot{q}_d \quad (53)$$

System output $y = h(x)$ for this approach is chosen as a switching function (s) constituting the sliding line in the phase space.

$$y = s(\dot{q}_e, q_e) \quad (54)$$

$$s := \dot{q}_e + \beta q_e \quad (55)$$

where the parameter β is chosen as below to make the switching function (s) Hurwitz.

$$\beta = \text{diag}(\beta_\theta \quad \beta_\psi), \quad \beta_\theta > 0, \beta_\psi > 0 \quad (56)$$

The selection in (54) when maintained at zero provides the sliding mode property to the passivity-based control system. Chosen storage function candidate is

$$V := \frac{1}{2} s^T D s \quad (57)$$

which is positive definite and its derivative can be evaluated as in (58) considering (53) and (55).

$$\begin{aligned} \dot{V} &= s^T D \dot{s} + \frac{1}{2} s^T \dot{D} s \\ &= s^T \left(D \dot{s} + \frac{1}{2} \dot{D} s \right) \\ &= s^T \left(D \dot{q}_e + D \beta \dot{q}_e + \frac{1}{2} \dot{D} \dot{q}_e + \frac{1}{2} \dot{D} \beta q_e \right) \\ &= s^T \left(\tau - G(q) - D \ddot{q}_d - C \dot{q}_d - B \dot{q}_d - C \dot{q}_e - B \dot{q}_e + D \beta \dot{q}_e + \frac{1}{2} \dot{D} \dot{q}_e + \frac{1}{2} \dot{D} \beta q_e \right) \\ &= s^T \left(\tau - G(q) - D \ddot{q}_d - (B + C) \dot{q} + D \beta \dot{q}_e + \frac{1}{2} \dot{D} \dot{q}_e + \frac{1}{2} \dot{D} \beta q_e \right) \\ &= s^T \left(\tau - G(q) - (B + C) \dot{q} + D(\beta \dot{q}_e - \ddot{q}_d) + \frac{1}{2} \dot{D}(\dot{q}_e + \beta q_e) \right) \end{aligned} \quad (58)$$

At this step, the appropriate τ choice is

$$\tau := G(q) + (B + C) \dot{q} - D(\beta \dot{q}_e - \ddot{q}_d) - \frac{1}{2} \dot{D}(\dot{q}_e + \beta q_e) + v \quad (59)$$

where the variable v is a newly defined virtual input. Accordingly, the derivative of storage function given in (58) takes the form below.

$$\dot{V} = s^T v \quad (60)$$

The fictitious control term v is determined as

$$v = -\omega \text{sat}(s) - \gamma \tan^{-1}(s) \quad (61)$$

where $\text{sat}(s)$ is the saturation function defined to limit s with a positive constant ϕ as below.

$$\text{sat}(s) = \begin{cases} \phi & \text{if } s > \phi \\ s & \text{if } s \leq \phi \end{cases}, \quad \phi = \begin{bmatrix} \phi_\theta \\ \phi_\psi \end{bmatrix}, \quad \phi_\theta > 0, \phi_\psi > 0 \quad (62)$$

The choice above affects the control signal when a decrease in the pitch angle is commanded. Due to the gravity, helicopter pitch angle decreases by itself and a limit is imposed to at a level of 0.23 to keep the main motor on. The effect of an upper bounding saturation in (51) has no effect in the cases where the helicopter pitch angle increases. The other parameters describing v are

$$\begin{aligned} \gamma &= \text{diag}(\gamma_\theta \quad \gamma_\psi), \quad \gamma_\theta > 0, \quad \gamma_\psi > 0 \\ \omega &= \text{diag}(\omega_\theta \quad \omega_\psi), \quad \omega_\theta > 0, \quad \omega_\psi > 0 \end{aligned} \quad (63)$$

Rewriting (60) with the fictitious control input in (61) yields the following derivative;

$$\dot{V} = -s^T (\omega \text{sat}(s) - \gamma \tan^{-1}(s)) \leq 0 \quad (64)$$

which satisfies the inequalities (65),(66) and (67) of being a passive system with the output $y = s$ and the input $v = -\phi(y) = -\omega \text{sat}(s) - \gamma \tan^{-1}(s)$.

$$v^T y \geq \dot{V} \quad (65)$$

$$y^T \phi(y) > 0, \quad \forall y \neq 0 \quad (66)$$

$$\phi(0) = 0 \quad (67)$$

Moreover, when $v = 0$,

$$y \equiv 0 \Rightarrow s \equiv 0 \quad (68)$$

which indicates that the only solution providing the system output as zero is $s = 0$. A single point solution ($q = 0, \dot{q} = 0$) is entailed for zero state observability, however in this case a set including the required point is the solution. This solution set is a desired subspace designed by us in the phase space, and it forms the sliding line (s). It is known from SMC theory, when the error vector reaches the sliding line, it is going to converge to the origin ($q = 0, \dot{q} = 0$) which is also the required solution point. Therefore the ultimate solution is the origin of phase space and the system is zero state observable. By this way, the passivity of the system is ensured between the input v and the switching function (s) by using state feedback as discussed by [Byrnes et al., 1991]. Consequently, it is shown that the reaching of the error vector from any initial point to the desired subspace is globally stabilizable by the control input v . This methodology provides SMC to benefit from passivity for guiding the error vector to the desired subspace and holding it in the vicinity of there. As the last step of PB-SMC design, the overall control signal is obtained as given below.

$$u = g^{-1} \left(G(q) + (B+C)\dot{q} - D(\beta\dot{q}_e - \ddot{q}_d) - \frac{1}{2}\dot{D}(\dot{q}_e + \beta q_e) - \omega \text{sat}(s) - \gamma \tan^{-1}(s) \right) \quad (69)$$

where the inverse of $g(\theta)$ always exists. In the real time implementation, due to the effect of the gravity, the term $\tan^{-1}(s)$ used in (61) is limited between $(-\infty, 0.23]$ for pitch output and the hard limiters for the control signal are employed also in this scheme. The parameters involved in the design

are listed in Table 5 and the values have been refined after a set of experiments. The tracking task is performed for the same reference path as in previous sections and the tracking results of pitch and yaw are shown by Figures (15)-(16). The tracking performance of PB-SMC is satisfactory when the transient and steady state errors are taken into consideration. The results shown are achieved by visibly clear control signals for both axes.

Table 5: Parameter settings of PB-SMC scheme

Parameter	Explanation	Value
r		
γ_θ	Reaching law parameter of pitch angle	2
γ_ψ	Reaching law parameter of yaw angle	2
β_θ	The slope parameter of sliding line for pitch angle	1.1
β_ψ	The slope parameter of sliding line for yaw angle	2
ω_θ	Coefficient of switching function (s) for pitch angle	2
ω_ψ	Coefficient of switching function (s) for yaw angle	2
ϕ_θ	Upper limit of sat(s) for pitch angle	0.23
ϕ_ψ	Upper limit of sat(s) for yaw angle	∞

COMPARISON OF CONTROL METHODS

Real time performances of the implemented control schemes are compared under a set of measures tabulated in Table 6. Comparison is based on several criteria which are the quality of control signal, tracking error, steady state error and rise time. Tracking errors are quantified by their mean and variance values for each method and each axis. The quality of control signals are labeled as low, medium and high with regard to their smoothness.

Table 6: Comparison of controllers in terms of mean and variance values of tracking error and generated control signal

Angle type	Controller type	Tracking error		Rise time $t=60s$	Steady state error (deg) $t=60-65s$	Smoothness of control signal
		Mean	Variance			
Pitch angle	Fuzzy control	2.55	64.61	62.33	-0.3	L
	SMC	2.37	58.71	62.02	0.8	L
	Backstepping c.	2.70	68.74	61.73	0.5	M
	PB-SMC	2.38	58.96	61.59	0.4	H
Yaw angle	Fuzzy control	3.80	96.39	63.26	-0.2	H
	SMC	2.72	65.35	62.50	0.2	L
	Backstepping c.	2.95	67.41	63.14	0.3	M
	PB-SMC	2.61	62.23	61.96	0.2	M

Referring to the results in Table 6, one can see that PB-SMC and SMC approaches have the minimum tracking error values for the pitch angle. On the other hand, the control signal generated by PB-SMC has the highest smoothness. Backstepping controller also produces a smooth control signal, however it yields the largest error mean for the pitch angle. PB-SMC reached to lower error levels with a clear control signal; therefore the performance of passivity based approach is prominent in the pitch angle. For the control of the yaw angle, SMC and PB-SMC are again the best performing schemes. PB-SMC achieves the minimum values for the mean and variance of the tracking errors. Backstepping controller produces higher tracking error; nevertheless the control signal is smooth enough. Likewise, the control signal of fuzzy controller for yaw angle is the smoothest one, and apparently, the mean of tracking error of yaw angle has the highest value. When the reference trajectory for both axes is equal to 20 degrees and a rising pulse is applied, i.e. $t \in [60 \ 70]$ sec., shortest rising times are observed for the backstepping control and PB-SMC for pitch angle. For yaw angle, SMC and PB-SMC yield a quicker climb toward the setpoint. Hence, one can see that PB-SMC is the best control scheme in terms of the small rising time criterion. Lowest steady state error for pitch angle is obtained by fuzzy control, and PB-SMC is the second. Steady state error of yaw angle is almost same for all control

strategies; however, the performance of backstepping controller is slightly poorer than the others. As a last comment, the chattering phenomenon observed for PB-SMC is significantly weaker than that in the SMC approach as the role of the signum term in PB-SMC technique is not the essential component as in the case of SMC.

CONCLUSIONS

Software centric control of processes is the recent trend on control engineering and practitioners frequently benefit from the possibilities offered by design platforms like Matlab to unfold interesting process responses and to observe desired behavior. The way to this goal is to design a software tool having a consistent mathematical basis as discussed in this paper. This paper focuses on several control schemes, including fuzzy control, backstepping control, SMC and PB-SMC, which are all software components coded appropriately. Fuzzy control has a linguistic structure overpassing the dynamical difficulties of systems. Backstepping technique is a good implementation of Lyapunov stability criterion which has an important place in control theory. Sliding mode control is known with its robustness against disturbances and parameter uncertainties. The last control technique included in this study is called passivity based sliding mode control obtained by defining the sliding mode control law under the circumstance that the passivity of the system is ensured. The first three methods are chosen to compare different philosophies which have high reputation in control theory. The last control scheme proposed is incorporated into this comparison to develop the performance of SMC which gave better results than both fuzzy and backstepping techniques. The aim of the paper is to implement these techniques and perform real time tracking experiments on a 2-dof helicopter, known for its high non-linearity and the coupling between its axial motions. The tracking task is accomplished parallel to the expectations put forth theoretically and a comparison is made. The tracking errors and control signals are checked for all schemes. According to the metrics considered in the comparison work, PB-SMC approach has displayed the most desired closed loop control features.

The results of the comparison justify the strength of SMC approach against disturbances and parametric uncertainties. The incorporation of passivity approach into SMC yields a more powerful control scheme (PB-SMC). While the robustness of SMC is preserved, the well known weakness, called chattering, of SMC is improved. Accordingly the control signal quality is increased in terms of its smoothness. In conclusion, though all controllers perform well in accurate tracking criterion, sliding mode based approaches produce the best results. Overall, the paper contributes an in-depth performance comparison of several nonlinear control techniques on a real time nonlinear system and offers PB-SMC as the most desirable control technique.

References

- Agudelo OM, Espinosa JJ and Vandewalle J. (2007) *Control of a helicopter laboratory process using fuzzy techniques* 2007. Internal Report 06-74.
- Ahmad SM, Chipperfield AJ and Tokhi MO.(2003) *Dynamic modelling and linear quadratic gaussian control of a twin-rotor multi-input multi-output system*. Proc. of The Institution of Mechanical Engineers Part I-Journal of Systems and Control Engineering 2003; 217: 203-227.
- Bridges MM, Dawson DM and Abdallah CT. (1995) *Control of rigid-link, flexible-joint Robots - a survey of backstepping methods*. Journal of Robotic Systems 1995; 12:199-216.
- Byrnes CI, Isidori A and Willems JC. (1991) *Passivity, feedback equivalence, and the global stabilization of minimum phase nonlinear-systems*. IEEE Trans. on Automatic Control 1991; 36: 1228-1240.
- Das A, Lewis F and Subbarao K. (2009) *Backstepping approach for controlling a quadrotor using Lagrange form dynamics*. Journal of Intelligent & Robotic Systems 2009; 56: 127-151.
- Efe MÖ. (2008) *Fractional fuzzy adaptive sliding-mode control of a 2-dof direct-drive robot arm*. IEEE Trans. on Systems Man and Cybernetics Part B-Cybernetics 2008; 38: 1561-1570.

- Ertuğrul M, Kaynak O, Sabanovic A and Ohnishi K. (1996) *Generalized approach for Lyapunov design of sliding mode controllers for motion control applications*. 4th Int. Workshop on Advanced Motion Control 1996; 1-2: 407-412.
- Frazzoli E, Dahleh MA and Feron E. (2000) *Trajectory tracking control design for autonomous helicopters using a backstepping algorithm*. Proc. of the 2000 American Control Conference, 1-6: 4102-4107.
- Freeman RA. (2008) *Robust Nonlinear Control Design: State-Space and Lyapunov Techniques* 2008 Boston, MA, Birkhaeuser.
- Juang JG, Lin RW and Liu WK. (2008) *Comparison of classical control and intelligent control for a mimo system*. Applied Mathematics and Computation 2008; 205: 778-791.
- Juang JG, Huang MT and Liu WK. (2008) *PID control using presearched genetic algorithms for a mimo system*. IEEE Transactions on Systems Man and Cybernetics Part C-Applications and Reviews 2008; 38: 716-727.
- Khalil HK. (2002) *Nonlinear Systems*, 2002 NJ, Prentice Hall.
- Koshkouei AJ. (2008) *Passivity-based sliding mode control for nonlinear systems*. Int. J of Adaptive Control and Signal Processing 2008; 22: 859-874.
- Krstic M, Kanellakopoulos I. and Kokotovic PV. (1995) *Nonlinear and Adaptive Control Design* 1995 New York, Wiley.
- Lopez-Martinez, M, Vivas C and Ortega MG. (2005) *A multivariable nonlinear h-infinity controller for a laboratory helicopter*. 44th IEEE Conference on Decision and Control & European Control Conference 2005; 1-8: 4065-4070.
- Lopez-Martinez M, Ortega MG, Vivas C and Rubio FR. (2007) *Nonlinear L-2 control of a laboratory helicopter with variable speed rotors*. Automatica 2007, 43: 655-661.
- Ma H, Xu F, Du L and Chen XB. (2009) *Discrete-time passivity-based sliding-mode control of single-phase current-source inverter*. 35th Annual Conf. of IEEE Industrial Electronics 2009; 1-6: 369-373
- Mendel JM. (2001) *Uncertain rule-based fuzzy logic systems: introduction and new directions*, 2001 Prentice Hall Ptr.
- Ortega R. (1998) *Passivity-Based Control of Euler-Lagrange Systems: Mechanical, Electrical, and Electromechanical Applications* 1998 New York, Springer.
- Quanser Inc. (2006) *Quanser 2 dof helicopter user and control manual* 2006; Revision 1. 119 Spy Court Markham, Ontario L3R 5H6 Canada.
- Rahideh A and Shaheed MH. (2009) *Real time hybrid fuzzy-pid control of a twin rotor system*. IEEE Int. Conf. on Mechatronics 2009; 1-2; 327-332.
- Rahideh A and Shaheed MH. (2007) *Mathematical dynamic modelling of a twin-rotor multiple input-multiple output system*. Proceedings of The Institution of Mechanical Engineers Part I-Journal of Systems and Control Engineering 2007; 221: 89-101.
- Roopaei M and Jahromi MZ. (2008) *Synchronization of two different chaotic systems using novel adaptive fuzzy sliding mode control* 2008; Chaos 18:033133.

- Shaik FA and Purwar S. (2009) *A nonlinear state observer design for 2-DOF twin rotor system using neural networks*. Int. Conf. on Advances in Computing, Control, & Telecommunication Technologies 2009; 15-19.
- Su JP, Liang CY and Chen HM. (2002) *Robust control of a class of nonlinear systems and its application to a twin rotor mimo system*. IEEE Int. Conf. on Industrial Technology 2002; I-II: 1272-1277.
- Subudhi B and Jena D. (2009) *Nonlinear system identification of a twin rotor mimo system*. 2009 IEEE Region 10 Conference 1-4: 437-442.
- Tao CW, Taur JS, Chang YH and Chang CW. (2010) *A novel fuzzy sliding and fuzzy integral sliding controller for the twin rotor multi-input multi-output system*. IEEE Trans. on Fuzzy Systems 2010; 18:893-905.
- Toha SF and Tokhi MO. (2010) *Parametric modelling application to a twin rotor system using recursive least squares, genetic, and swarm optimization techniques*. Proc. of the Institution of Mechanical Engineers Part G-Journal of Aerospace Engineering 2010. 224 (G9): 961-977.
- Tokat S, Eksin İ, Güzelkaya M. (2009) *Linear time-varying sliding surface design based on co-ordinate transformation for high-order systems*. Transactions of The Institute of Measurement and Control 2009; 31: 51-70.
- Utkin VI, Guldner J and Shi J. (2009) *Sliding Mode Control in Electromechanical Systems*. 2009; London, Taylor & Francis.
- Wang WJ and Chen JY. (2005) *Passivity-based sliding mode position control for induction motor drives*. IEEE Trans. on Energy Conversion 2005; 20: 316-321.
- Yu GR. (2007) *Robust-optimal control of a nonlinear two degree-of-freedom helicopter*. 6th IEEE/ACIS Int. Conf. on Computer and Information Science 2007, 744-749.
- Yu X and Kaynak O. (2009) *Sliding-mode control with soft computing: a survey*. IEEE Trans. on Industrial Electronics 2009; 56: 3275-3285.
- Yang JH and Hsu WC. (2009) *Adaptive backstepping control for electrically driven unmanned helicopter*. Control Engineering Practice 2009; 17: 903-913.

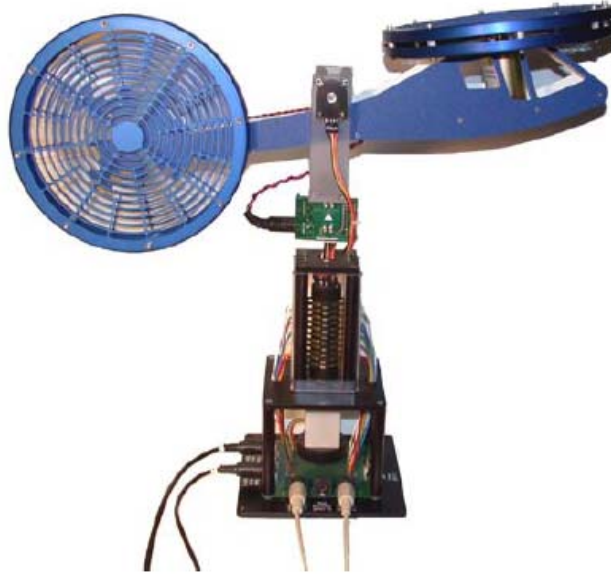


Figure 1: 2-DOF Helicopter

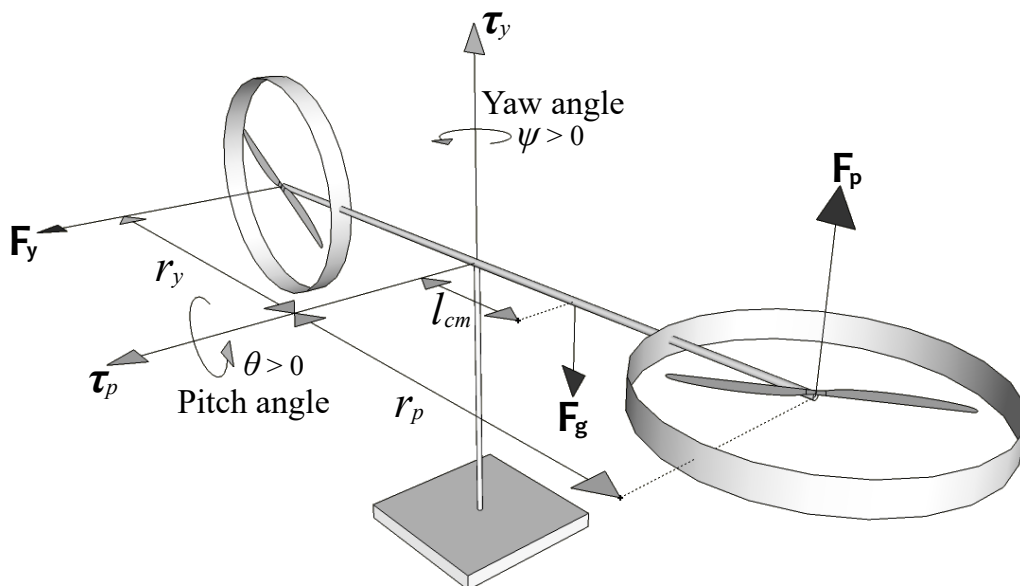


Figure 2: Dynamic model of 2-DOF Helicopter

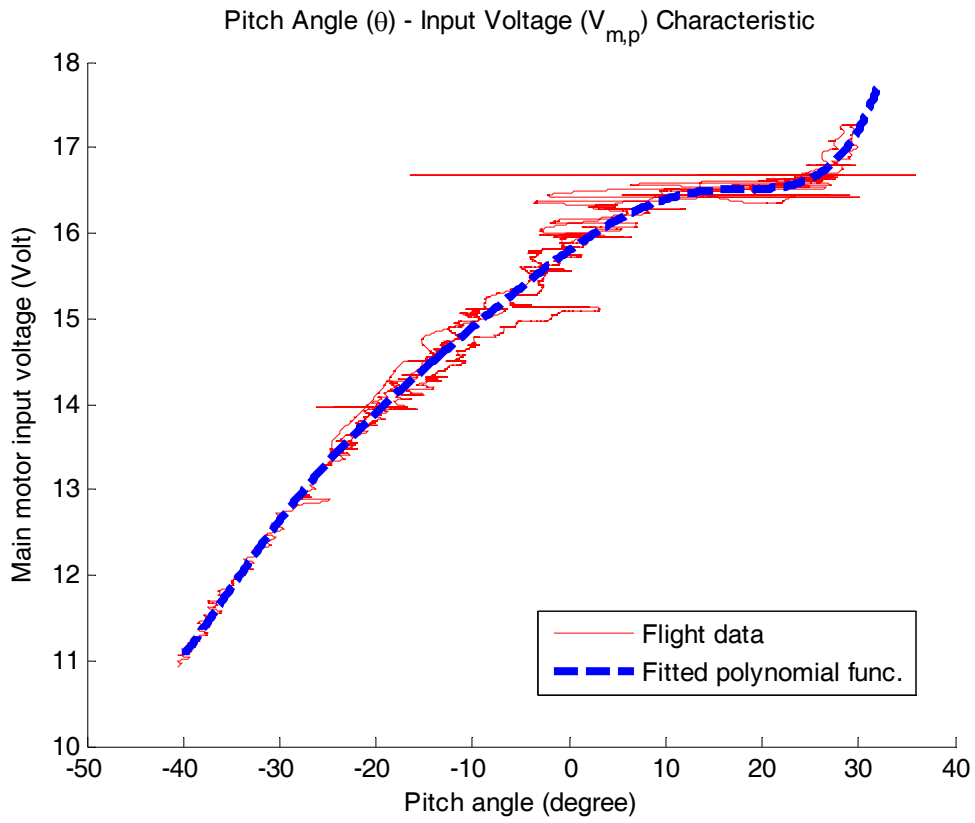


Figure 3: Steady state pitch angle – Main motor voltage input curve

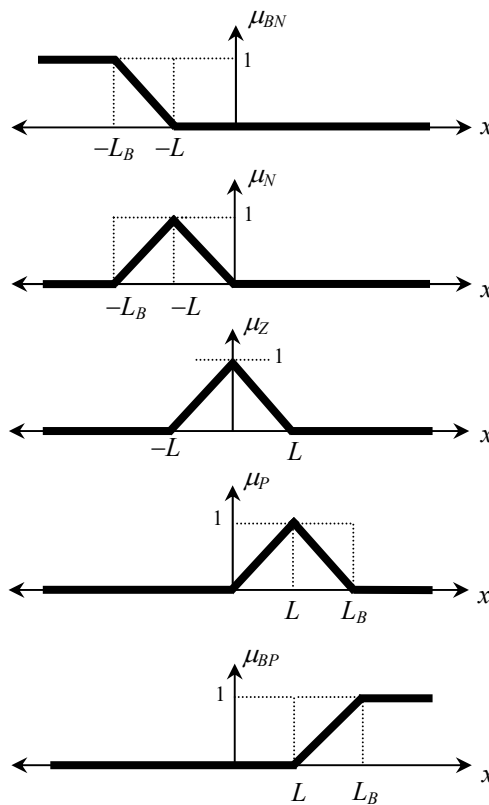


Figure 4: Membership functions

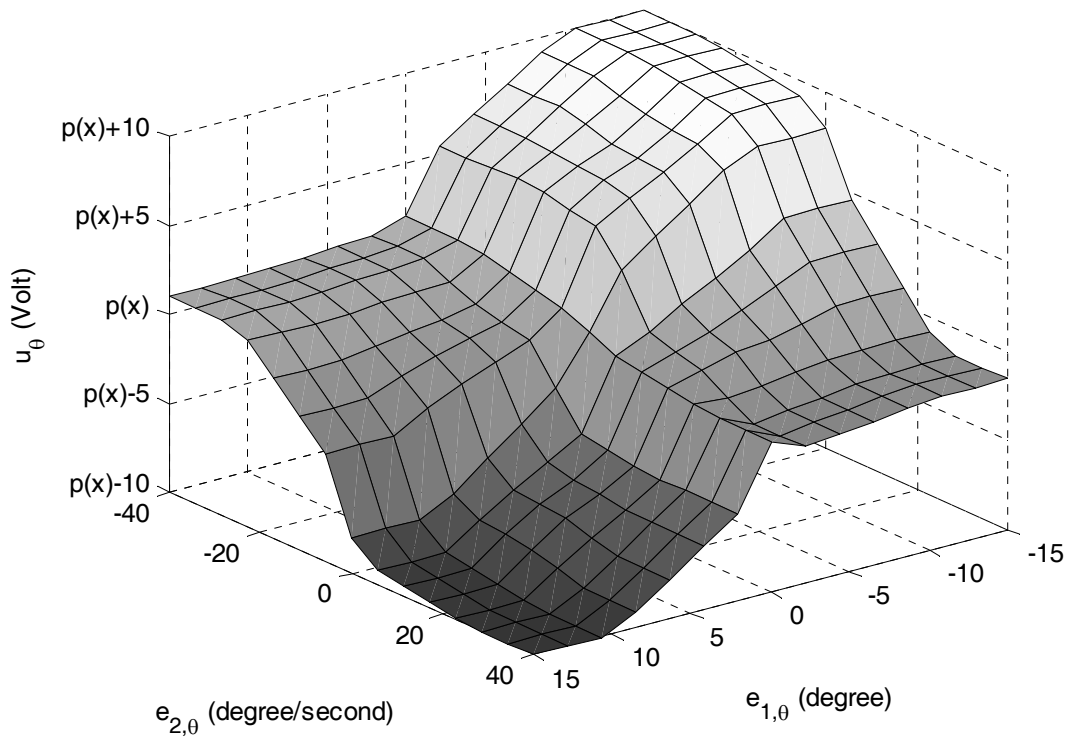


Figure 5: Control surface of the pitch angle fuzzy system

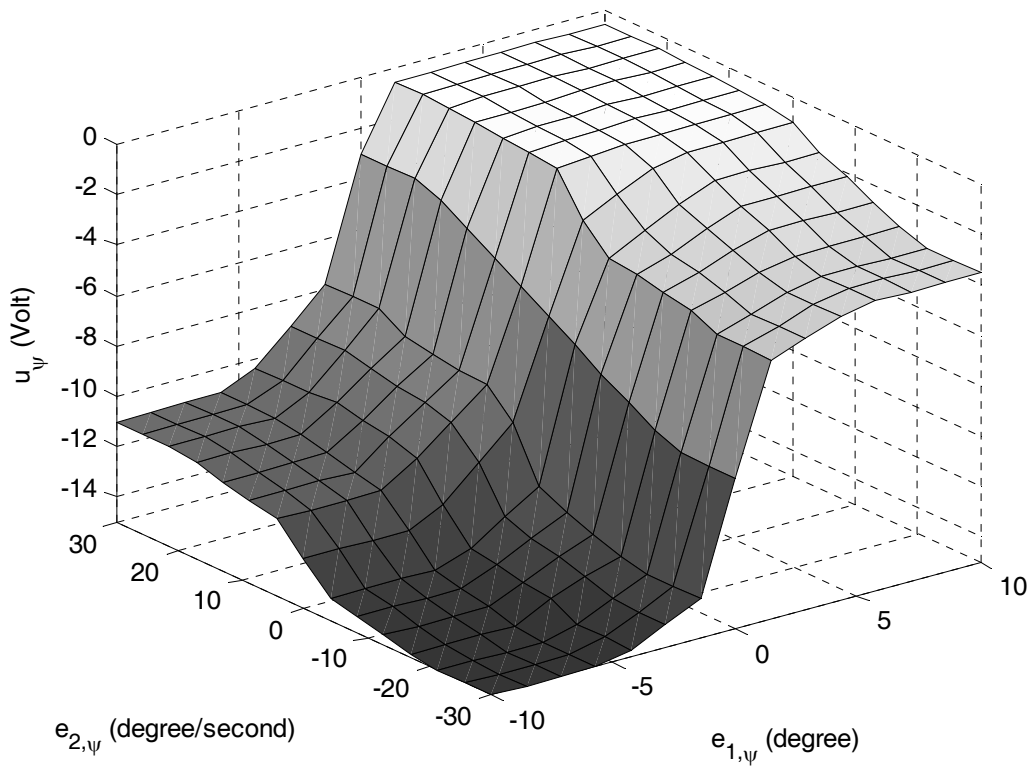


Figure 6: Control surface of the yaw angle fuzzy system

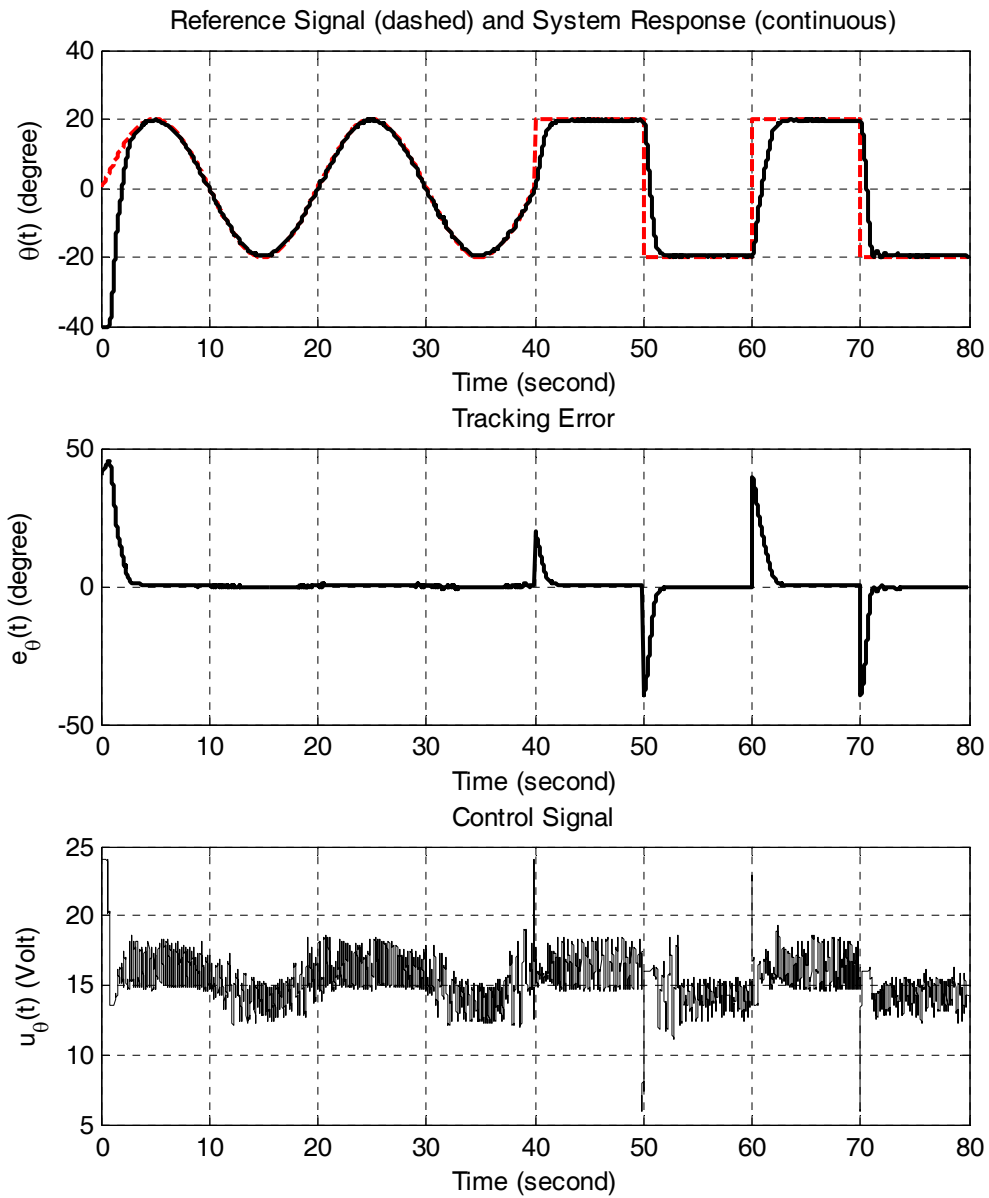


Figure 7: Pitch angle tracking (top), tracking error (middle) and control signal generated by the fuzzy controller (bottom).

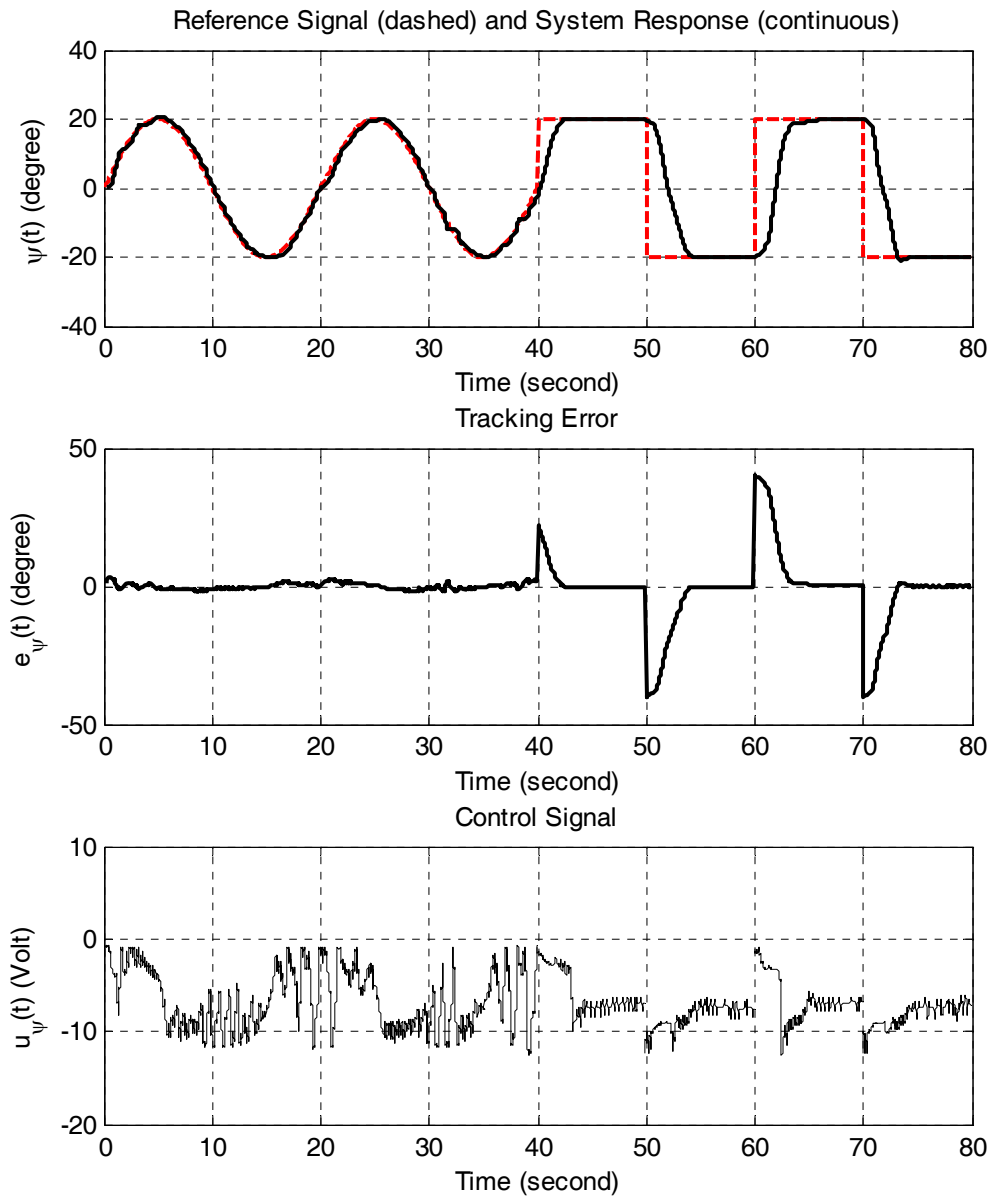


Figure 8: Yaw angle tracking (top), tracking error (middle) and control signal generated by the fuzzy controller (bottom).

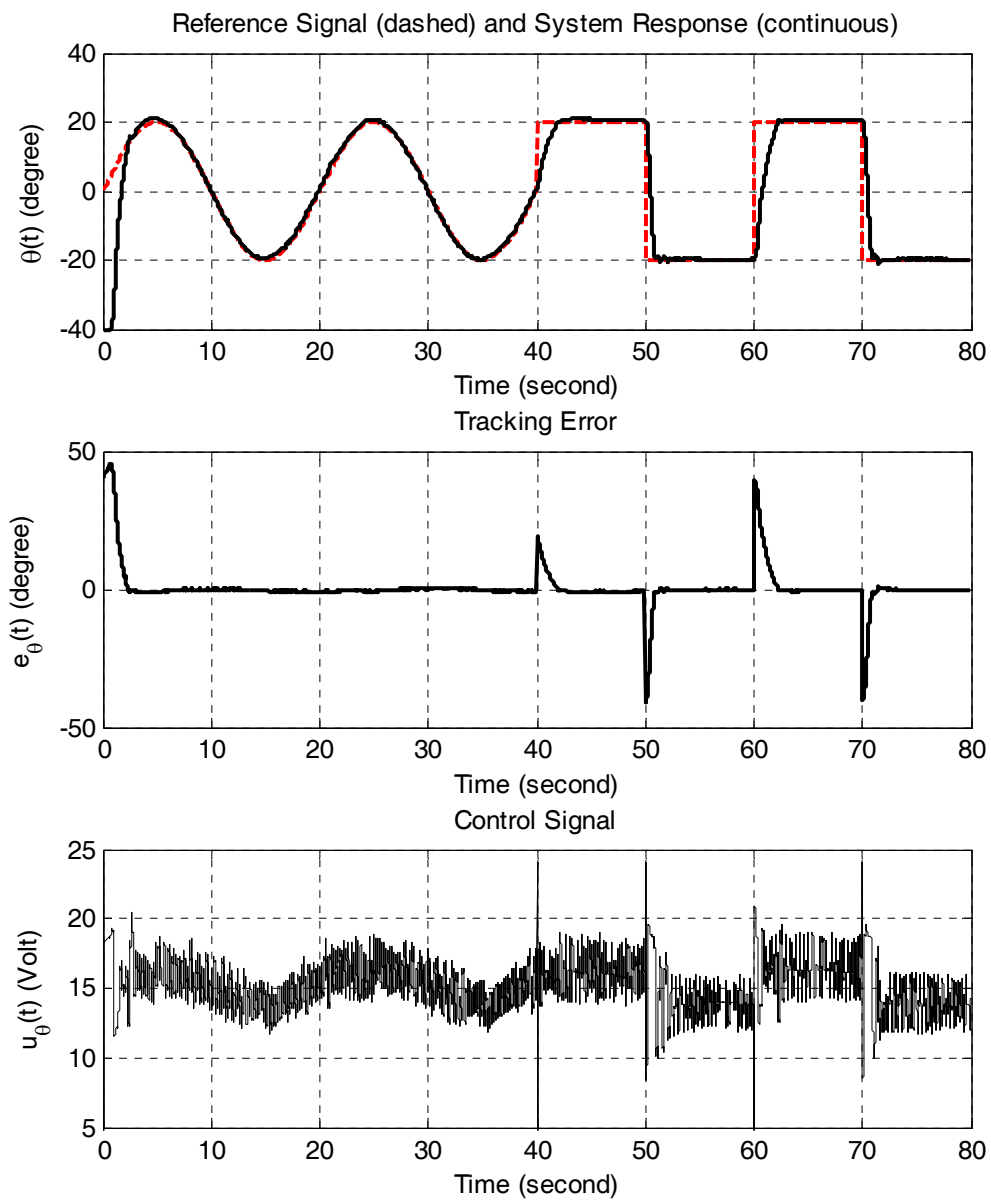


Figure 9: Pitch angle tracking (top), tracking error (middle) and control signal generated by the sliding mode controller (bottom).

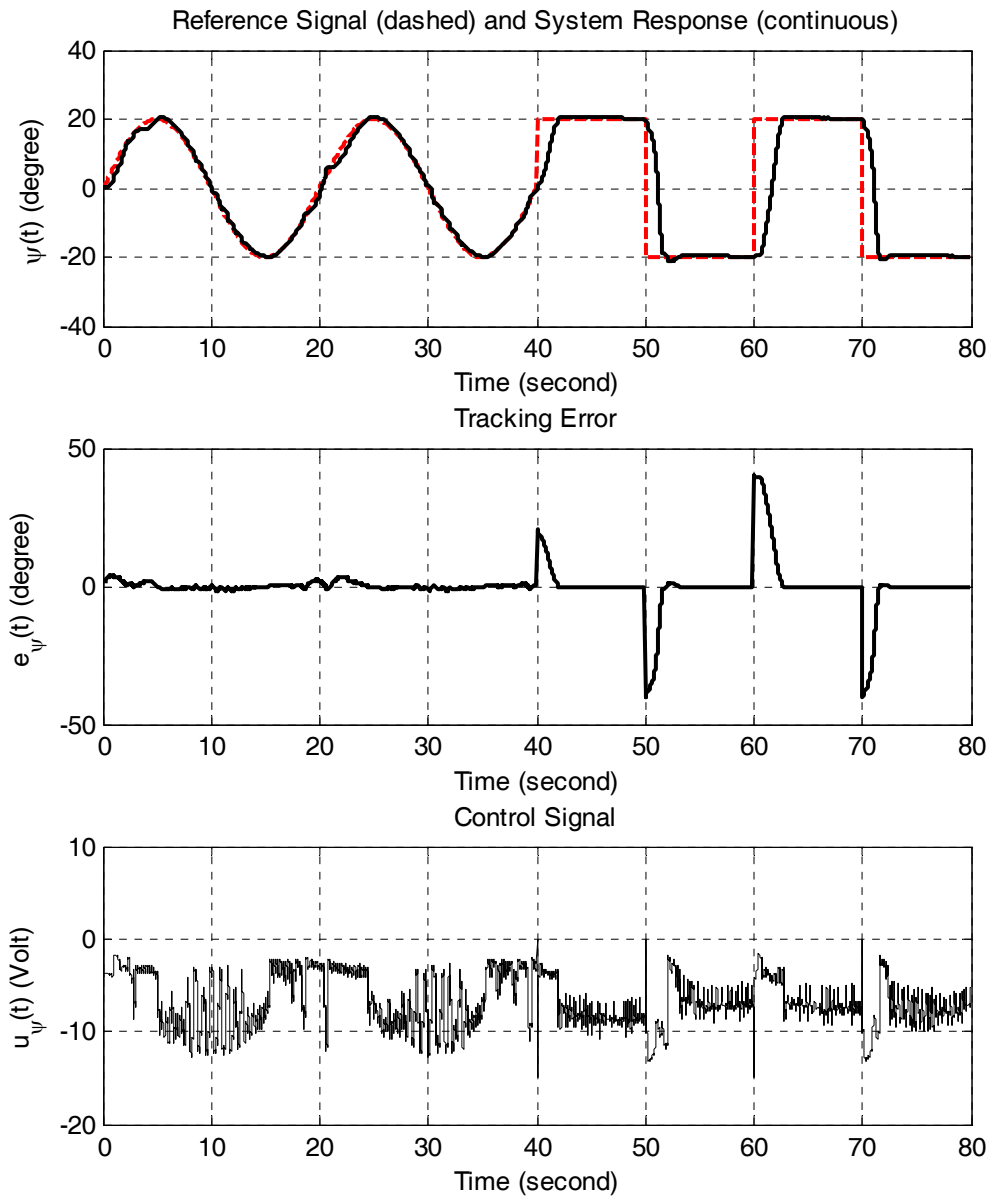


Figure 10: Yaw angle tracking (top), tracking error (middle) and control signal generated by the sliding mode controller (bottom).

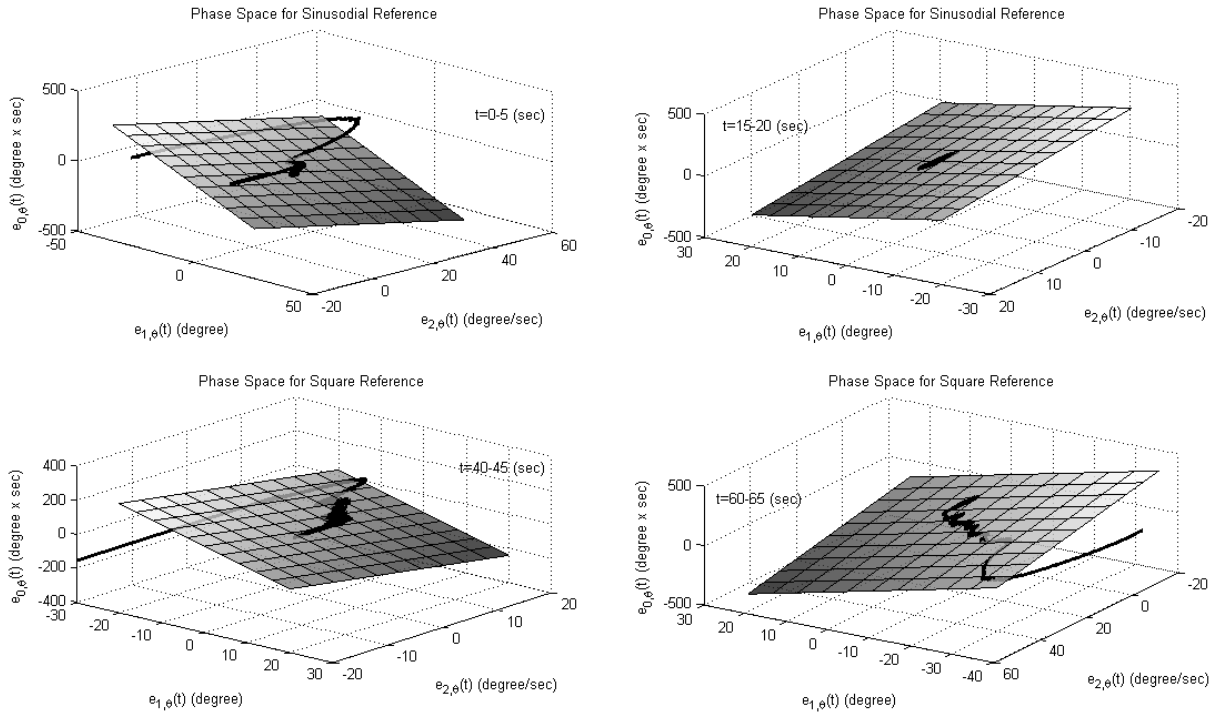


Figure 11: The error vector trajectory corresponding to pitch angle in the phase space for different periods of real time application.

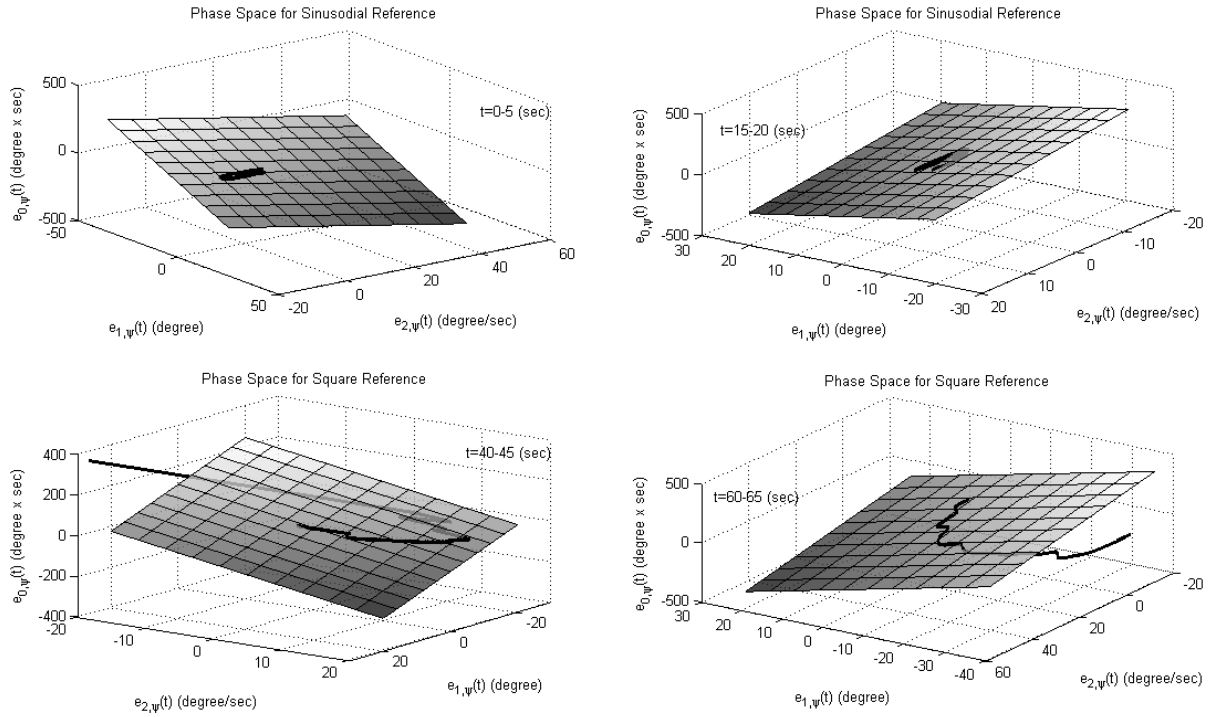


Figure 12: The error vector trajectory corresponding to yaw angle in the phase space for different periods of real time application.

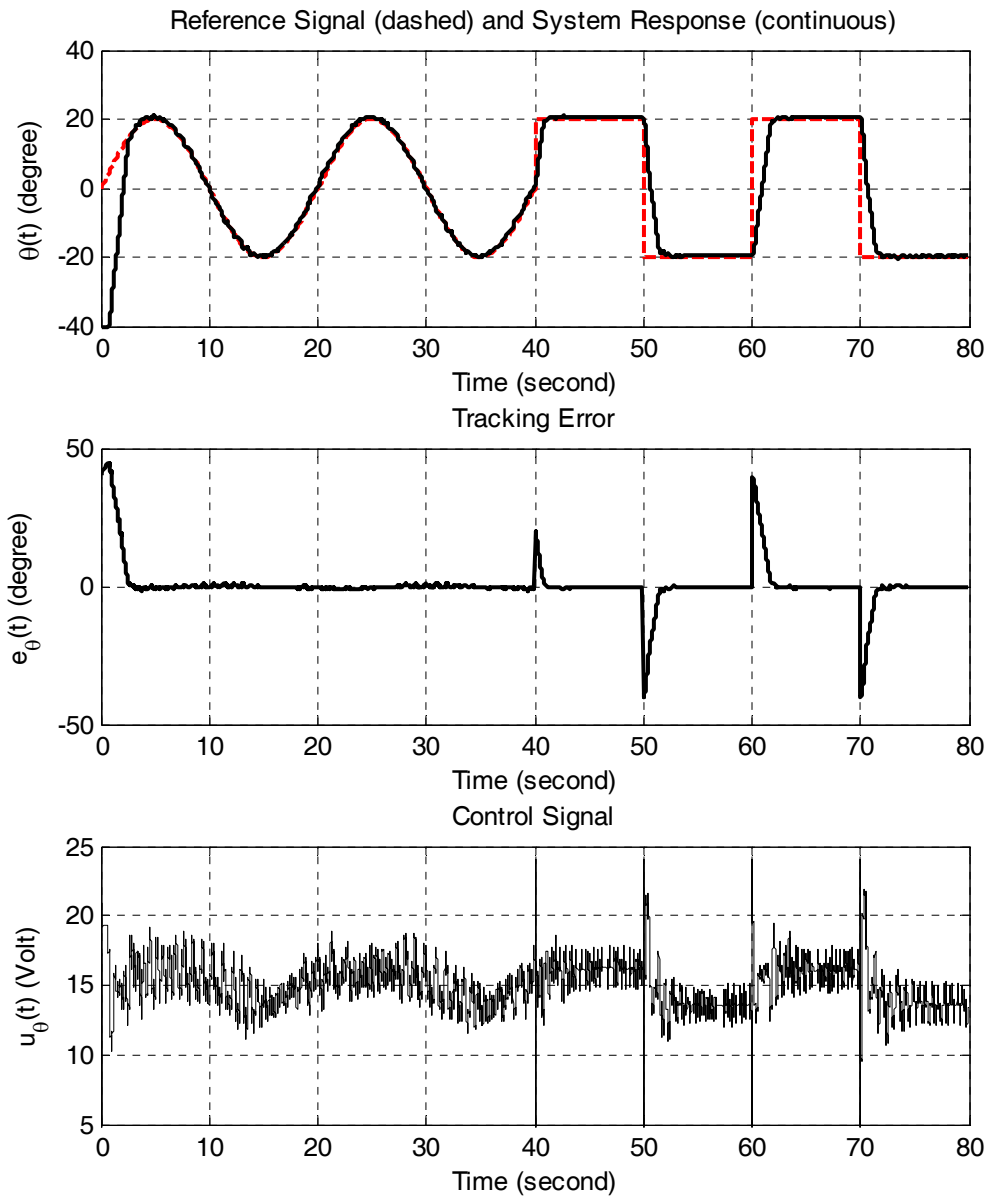


Figure 13: Pitch angle tracking (top), tracking error (middle) and control signal generated by the backstepping controller (bottom).

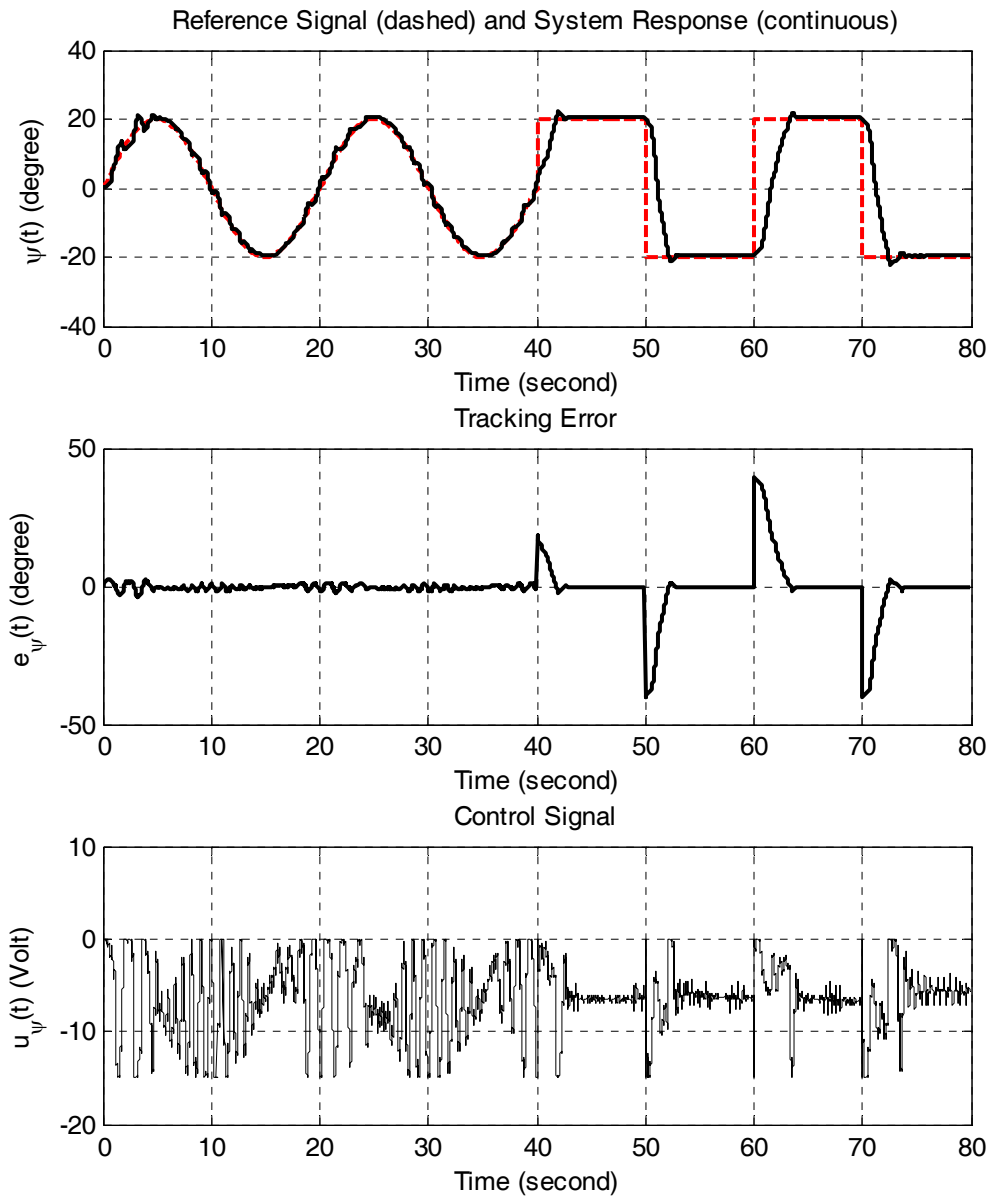


Figure 14: Yaw angle tracking (top), tracking error (middle) and control signal generated by the backstepping controller (bottom).

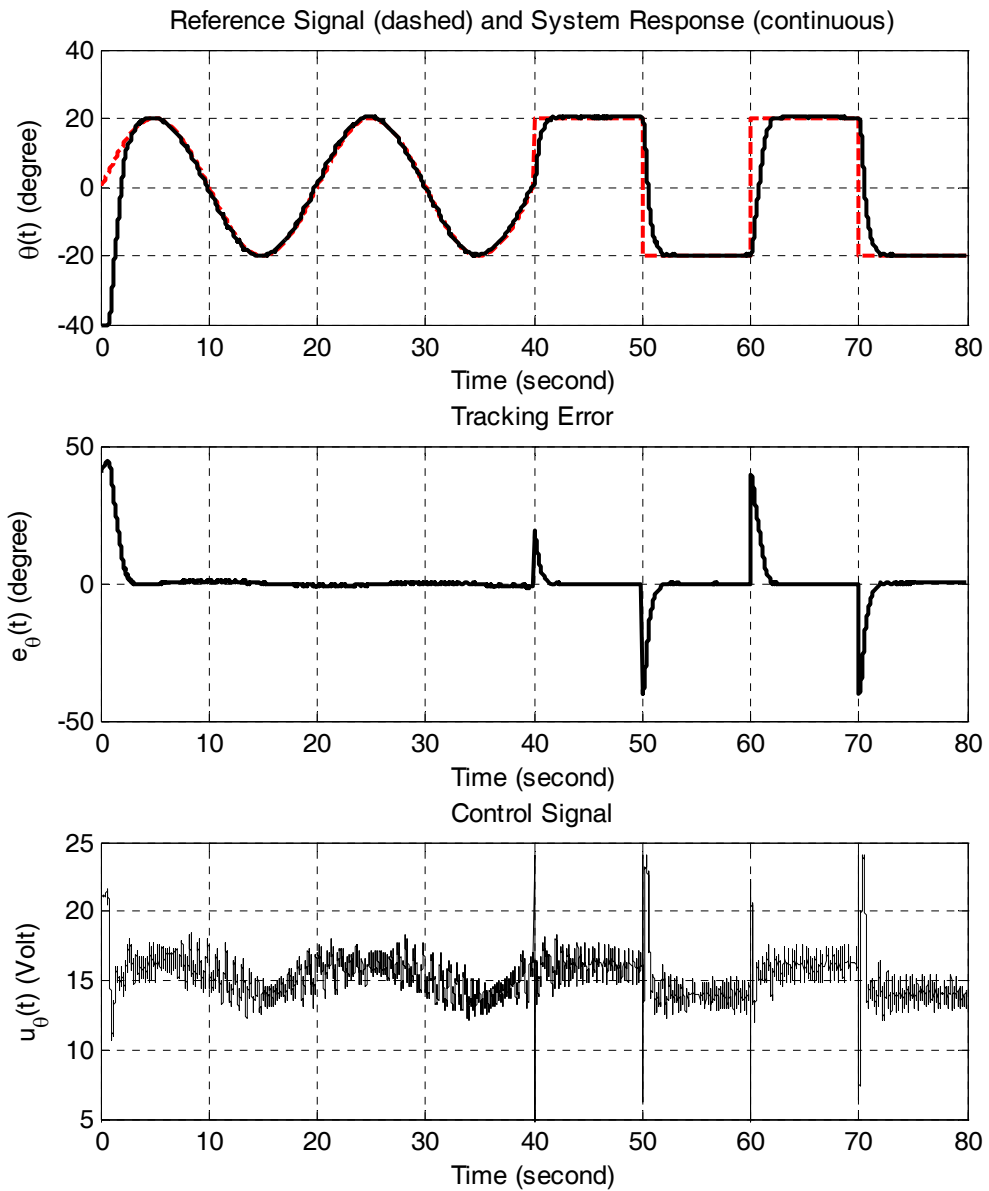


Figure 15: Pitch angle tracking (top), tracking error (middle) and control signal generated by the PB-SMC (bottom).

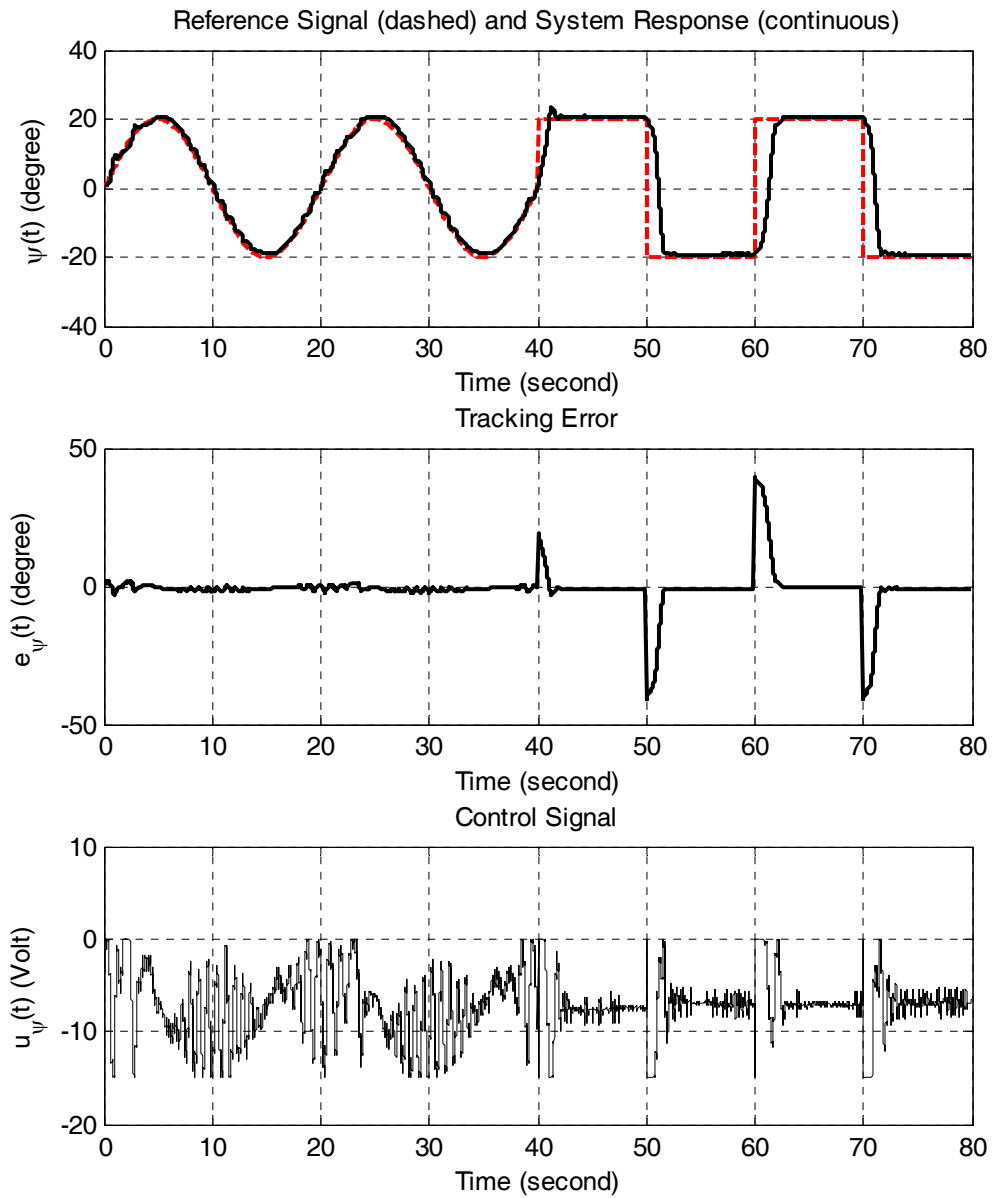


Figure 16: Yaw angle tracking (top), tracking error (middle) and control signal generated by the PB-SMC (bottom).